Variable Projection Order Adaptive Filtering Algorithm for Self-interference Cancellation in Airborne Radars

LI Haorui[1], *GAO Ying*[1], *GUO Xinyu*[2], *OU Shifeng*[1*]

1. College of Physics and Electronic Information, Yantai University, Yantai 264005, P. R. China;
2. Key Laboratory of Geophysical Exploration Equipment, Ministry of Education, College of Instrumentation and Electrical Engineering, Jilin University, Changchun 130000, P. R. China

(Received 20 June 2025; revised 7 August 2025; accepted 15 August 2025)

Abstract: The adaptive filtering algorithm with a fixed projection order is unable to adjust its performance in response to changes in the external environment of airborne radars. To overcome this limitation, a new approach is introduced, which is the variable projection order Ekblom norm-promoted adaptive algorithm (VPO-EPAA). The method begins by examining the mean squared deviation (MSD) of the EPAA, deriving a formula for its MSD. Next, it compares the MSD of EPAA at two different projection orders and selects the one that minimizes the MSD as the parameter for the current iteration. Furthermore, the algorithm's computational complexity is analyzed theoretically. Simulation results from system identification and self-interference cancellation show that the proposed algorithm performs exceptionally well in airborne radar signal self-interference cancellation, even under various noise intensities and types of interference.

Key words: adaptive filtering algorithm; airborne radar; variable projection order; mean squared deviation; self-interference cancellation

CLC number: V243 **Document code:** A **Article ID:** 1005-1120(2025)04-0497-12

0 Introduction

Airborne radars play an important role in modern military and civilian applications, particularly in meteorological monitoring, aviation navigation, and target detection. Researchers have proposed self-interference cancellation techniques to suppress interference between the signals emitted by airborne radar and the received echo signals, thereby improving the performance of airborne radar. Adaptive filtering algorithms, with their fast and flexible characteristics, have been widely applied in the field of self-interference cancellation for airborne radar[1-5]. Among these, the least mean square (LMS) algorithm based on the minimum mean square error (MSE) criterion, as well as the normalised least mean square (NLMS) algorithm, which does not require extensive data training, have been particularly favoured[6-8]. With the introduction of the affine projection (AP) algorithm, the significant progress has been made in improving convergence speed by reusing input signals[9]. In addition, the recursive least square (RLS) algorithm based on least square estimation utilises all observation data from the initial time to the current time through the filter, thereby demonstrating stronger simulation capabilities for the coefficient vector of self-interference channels. It is widely used in self-interference cancellation technology for airborne radar signals[10].

However, the performance of the above algorithm deteriorates significantly under interference from complex environments such as high-intensity pulse noise signals. Therefore, they cannot be applied to airborne radar signal processing in complex

*Corresponding author, E-mail address: ousfeng@ytu.edu.cn.

How to cite this article: LI Haorui, GAO Ying, GUO Xinyu, et al. Variable projection order adaptive filtering algorithm for self-interference cancellation in airborne radars[J]. Transactions of Nanjing University of Aeronautics and Astronautics, 2025, 42(4):497-508.

http://dx.doi.org/10.16356/j.1005-1120.2025.04.006

environments[11]. To improve the robustness of algorithms in complex environments, some researchers have proposed the affine projection symbol (APS) algorithm by combining the cost functions of the symbolic algorithm (SA) and the AP algorithm, demonstrating superior pulse noise adaptability[12-15]. Recently, researchers have proposed the Ekblom promoted adaptive algorithm (EPAA) based on the Ekblom norm. This method enables the algorithm to maintain high robustness while keeping low computational complexity[16-17]. Additionally, the echo cancellation simulation environment of this algorithm closely resembles the self-interference cancellation environment[18-19]. Furthermore, researchers have proposed a variable step size (VSS) method based on the mean squared deviation (MSD) approach. This improvement enables the algorithm to achieve faster convergence while maintaining a low steady-state error level[20-21].

However, the current self-interference cancellation technology for airborne radars has high requirements for algorithm real-time performance and computational complexity[22-23]. Existing adaptive filtering algorithms struggle to achieve a balance between steady-state error, robustness, and computational complexity, which hinders their application in airborne radar signal processing under complex environmental conditions[24-26].

This paper proposes a variable projection order EPAA (VPO-EPAA). In each iteration of the algorithm, the optimal projection order is determined by comparing the mean square deviation (MSD) values of several projection orders, enabling the algorithm to maintain a fast convergence rate during the convergence phase and a low steady-state error during the steady-state phase. The proposed algorithm effectively addresses the trade-off between convergence speed and steady-state error while maintaining the high robustness of the original algorithm, and it also reduces computational complexity. Simulation results show that the algorithm performs excellently in self-interference elimination environments with different intensities and types of noise interference, and is suitable for applications in the field of airborne radar signal processing.

This paper consists of the following sections. Section 1 gives an overview of the existing base algorithms. Section 2 explains in detail the derivation process and implementation of the proposed algorithm in this paper. Section 3 compares and analyses the complexity of the algorithms. Section 4 carries out simulation experiments for the proposed algorithm and several sets of comparison algorithms from various perspectives. Section 5 concludes the paper.

1 Basic Principles

1.1 Algorithm model

The signals received by the receiver end of an airborne radar are typically composed of target echo signals, self-interference signals, and noise signals. To eliminate self-interference, a filter needs to be designed to separate the self-interference portion from the received signal using adaptive filtering technology[27-29]. This paper will use an improved adaptive filtering algorithm to simulate the self-interference channel of airborne radar signals in order to obtain the signals that need to be eliminated, facilitating subsequent precise cancellation processing. The desired signal simulated by the adaptive filtering algorithm can be expressed as

$$d(n)=\boldsymbol{x}^{\mathrm{T}}(n)\boldsymbol{w}_0+v'(n) \tag{1}$$

where $\boldsymbol{x}(n)=[x'(n),x'(n-1),\cdots,x'(n-L+1)]^{\mathrm{T}}$ is the input signal in the form of a vector, and L the total length of the system to be recognized and also the length of the adaptive filter; $\boldsymbol{w}_0=[w_1, w_2, \cdots, w_L]^{\mathrm{T}}$ is the weight vector of the self-interference path to be simulated; and $v'(n)$ the background noise. The error signal generated at each iteration is obtained by

$$e'(n)=d(n)-y(n)=d(n)-\boldsymbol{x}^{\mathrm{T}}(n)\boldsymbol{w}(n-1) \tag{2}$$

where $y(n)$ denotes the output signal of each iteration and $\boldsymbol{w}(n)$ the weight vector produced by each iteration. The ultimate goal of the algorithm is to make $\boldsymbol{w}(n)$ constantly approach $\boldsymbol{w}_0$ to achieve the simulation of the self-interference channel.

1.2 EPAA implementation

EPAA is a commonly used adaptive filtering al-

gorithm. The algorithm is highly robust and suitable for acoustic echo cancellation and self-interference cancellation in airborne radar signals. The algorithm reuses the input data following a similar approach to affine projection. The cost function of this algorithm is defined using the Ekblom norm, shown as

$$J_{\mathrm{EPAA}}(n)=\frac{1}{q}\sum_{i=0}^{P-1}(e^2(n-i)+m^2)^{\frac{q}{2}} \tag{3}$$

where q is the tuning parameter; P the order of data reuse, also known as the projection order; and m the small regularization constant. The algorithm's iterative formulation is derived through gradient descent

$$\boldsymbol{w}(n)=\boldsymbol{w}(n-1)+\mu\boldsymbol{X}(n)\boldsymbol{H}(n)\boldsymbol{e}(n) \tag{4}$$

where input signal matrix is defined as $\boldsymbol{X}(n)=[\boldsymbol{x}(n),\boldsymbol{x}(n-1),\cdots,\boldsymbol{x}(n-K+1)]^{\mathrm{T}}$; The error signal in vector form is represented as $\boldsymbol{e}(n)=[e'(n),e'(n-1),\cdots,e'(n-K+1)]^{\mathrm{T}}$; The algorithm's step size is denoted by μ; and $\boldsymbol{H}(n)$ is a diagonal matrix with size of $K\times K$, given by $\boldsymbol{H}(n)=\mathrm{diag}\,[h(n),h(n-1),\cdots,h(n-K+1)]$. Its diagonal elements are shown as

$$h_k(n)=(e'^2(n-k+1)+m^2)^{\frac{q-2}{2}}$$
$$k=1,2,\cdots,K \tag{5}$$

When significant errors are caused by impulsive noise, $h_k(n)$ quickly decreases to reduce the influence of large error signals on the algorithm. This gives the algorithm strong robustness in complex environments.

2 VPO-EPAA and Its Implementation

Conventional EPAA belongs to acoustic echo cancellation algorithms, which use scenarios and self-interference cancellation of airborne radar signals similar to those in scenarios. However, if the original environment's speech signals are replaced with wider bandwidth airborne radar signals, and noise signals of different intensities or types are added to simulate complex environments, the steady-state error of the algorithm will increase, and its performance will be significantly reduced. To enable the algorithm to achieve a lower steady-state error and a faster convergence speed while maintaining low computational complexity, and to make it more suitable for radar signal processing scenarios, this paper introduces a variable projection order mechanism based on the original algorithm. This mechanism allows the algorithm to utilise more input signals in the initial stage to accelerate convergence, while using fewer input signals in the later steady-state stage to minimise steady-state error. Additionally, as the number of input signals used decreases, the computational complexity also gradually decreases.

This section will first study the MSD of the entire EPAA and obtain its calculation formula. Then, by comparing the MSD of two EPAAs with different projection orders, a switching mechanism for the EPAA projection order will be proposed.

The difference between the weight vector generated by each iteration of the algorithm and the desired weight vector can be defined by

$$\tilde{\boldsymbol{w}}(n)=\boldsymbol{w}_0-\boldsymbol{w}(n) \tag{6}$$

Combining Eq.(4) yields

$$\tilde{\boldsymbol{w}}(n)=\tilde{\boldsymbol{w}}(n-1)-\mu\boldsymbol{X}(n)\boldsymbol{H}(n)\boldsymbol{e}(n) \tag{7}$$

To eliminate the influence of $\boldsymbol{w}_0$ on the algorithm, the following formula is introduced as

$$\boldsymbol{\Phi}(n)=\boldsymbol{I}-\mu\boldsymbol{X}(n)\boldsymbol{H}(n)\boldsymbol{X}^{\mathrm{T}}(n) \tag{8}$$

Substituting Eq.(8) into Eq.(7) yields

$$\tilde{\boldsymbol{w}}(n)=\boldsymbol{\Phi}(n)\tilde{\boldsymbol{w}}(n-1)-\mu\boldsymbol{X}(n)\boldsymbol{H}(n)\boldsymbol{v}(n) \tag{9}$$

According to the definition of the autocorrelation matrix, when the iteration number is n, the MSD of the algorithm can be calculated as

$$\mathrm{MSD}(n)=E[\tilde{\boldsymbol{w}}(n)\tilde{\boldsymbol{w}}^{\mathrm{T}}(n)]\equiv Tr(\boldsymbol{P}(n))=p(n) \tag{10}$$

where E and Tr belong to the expectation operator and trace operator, respectively. Assume that the noise signal $\boldsymbol{v}(n)$ and the weight error vector from the previous iteration are statistically independent and follow the same distribution. The autocorrelation matrix of the weight error vector can be set as

$$\boldsymbol{P}(n)=E[\tilde{\boldsymbol{w}}(n)\tilde{\boldsymbol{w}}^{\mathrm{T}}(n)] \tag{11}$$

Substituting Eq.(9) into Eq.(11) yields

$$\boldsymbol{P}(n)=\boldsymbol{\Phi}(n)\boldsymbol{P}(n-1)\boldsymbol{\Phi}^{\mathrm{T}}(n)+\boldsymbol{D}(n) \tag{12}$$

$$\boldsymbol{D}(n)=\sigma_v^2\mu^2\boldsymbol{X}(n)\boldsymbol{H}(n)\boldsymbol{H}^{\mathrm{T}}(n)\boldsymbol{X}^{\mathrm{T}}(n) \tag{13}$$

Combining Eq.(10) and Eq.(12), the MSD of the algorithm can be expressed as

$$p(n)=Tr(\boldsymbol{\Phi}^{\mathrm{T}}(n)\boldsymbol{\Phi}(n)\boldsymbol{P}(n-1))+Tr(\boldsymbol{D}(n)) \tag{14}$$

As n approaches infinity, the weight vector parameters of the algorithm should be approximately equal to the parameters of the system to be simulated, and the error should be approximately zero. Combining Eqs.(11, 13, 14), the following limit can be obtained

$$\lim_{n\to+\infty} p(n)=\sigma_v^2\mu^2 Tr[\boldsymbol{X}(n)\boldsymbol{H}(n)\boldsymbol{H}^{\mathrm{T}}(n)\boldsymbol{X}^{\mathrm{T}}(n)] \tag{15}$$

Next, the projection order switching mechanism of this paper will be described. This mechanism selects a projection order scheme with a lower MSD value by comparing the $p(n)$ values of two EPAAs with different projection orders. The weight vector update formula of the algorithm proposed in this paper can be written as

$$\boldsymbol{w}(n)=\begin{cases}\boldsymbol{w}(n-1)+\mu\boldsymbol{X}_1(n)\boldsymbol{H}_1(n)\boldsymbol{e}_1(n)\\ \qquad p_1(n+1)\leqslant p_2(n+1)\\ \boldsymbol{w}(n-1)+\mu\boldsymbol{X}_2(n)\boldsymbol{H}_2(n)\boldsymbol{e}_2(n)\\ \qquad p_1(n+1)>p_2(n+1)\end{cases} \tag{16}$$

where $p_1(n+1)$ and $p_2(n+1)$ are the current estimates of MSD values of EPAA with orders K_1 and K_2, respectively; $\boldsymbol{X}_1(n)$ and $\boldsymbol{X}_2(n)$ the input matrices corresponding to the EPAA with different orders K_1 and K_2. Here, $K_1>K_2$ is set, which means that the EPAA with projection order K_1 has a faster convergence speed, while the EPAA with projection order K_2 has a lower steady-state error.

According to Eq.(14), the equations for calculating $p_1(n+1)$ and $p_2(n+1)$ in each iteration of EPAA are

$$p_1(n+1)=Tr(\boldsymbol{\Phi}_1^{\mathrm{T}}(n)\boldsymbol{\Phi}_1(n)\boldsymbol{P}_1(n))+Tr(\boldsymbol{D}_1(n)) \tag{17}$$

$$p_2(n+1)=Tr(\boldsymbol{\Phi}_2^{\mathrm{T}}(n)\boldsymbol{\Phi}_2(n)\boldsymbol{P}_2(n))+Tr(\boldsymbol{D}_2(n)) \tag{18}$$

Then, the equation for determining the MSD in the next iteration of the algorithm is

$$p(n+1)=\begin{cases}p_1(n+1) & p_1(n+1)\leqslant p_2(n+1)\\ p_2(n+1) & p_1(n+1)>p_2(n+1)\end{cases} \tag{19}$$

The iterative running processes of the VPO-EPAA algorithm proposed in this paper are as follows.

(1) Initialization: $\boldsymbol{w}(0)=[0,0,\cdots,0]_{1\times L}^{\mathrm{T}}$, $p_1(0)=p_2(0)=p(0)=1$, $\sigma_v^2=10^{-3}$. Parameters: μ, L, m, q, K_1, K_2.

(2) Calculate $p(n+1)$ for two different projection orders when computing the current iteration of EPAA.

(3) Select a K value that minimises the $p(n+1)$ value as the projection order for the current iteration of the algorithm.

(4) Update the value of $p(n+1)$ in the next iteration of the algorithm as shown in Eq.(19).

In terms of steady-state analysis, the step size range that allows EPAA to converge normally has been obtained using the energy conservation method[17], shown as

$$0<\mu<\frac{2m^{2-q}}{K\lambda_{\max}(\boldsymbol{R})} \tag{20}$$

$$\boldsymbol{R}=E[\boldsymbol{x}(n)\boldsymbol{x}^{\mathrm{T}}(n)] \tag{21}$$

According to Eq.(19), the projection order K of the algorithm will eventually stabilise at a pre-set smaller value (in most cases, 1). Therefore, the step size range of the algorithm proposed in this paper can be updated to

$$0<\mu<\frac{2m^{2-q}}{K_{\min}\lambda_{\max}(\boldsymbol{R})} \tag{22}$$

From Eq.(22), it can be seen that when determining the maximum value of the step size of the algorithm proposed in this paper, the size of the pre-set smaller projection order $K_{\min}$ should be considered.

3 Computational Complexity Analysis

This section compares the computational complexity of the proposed algorithm with that of other similar algorithms, such as affine projection algorithm (APA), affine projection symbol algorithm (APSA), VPO-APA[30], EPAA, VPO-proportionate afine projection algorithm (VPO-PAPA)[30], and VPO-EPAA. Table 1 presents a comparison of the number of multiplications and additions required per iteration for these algorithms. In Table 1, K_n reprents the variable projection order.

As can be seen from Table 1, the improvement in algorithm performance is likely achieved at the cost of increased computational complexity. The computational complexity of the proposed algorithm is intuitively higher than that of APSA and the original EPAA. However, due to the use of the VPO method, the projection order (K_n) in the proposed algorithm quickly becomes 1 and remains stable in most cases. In contrast, several comparison algorithms with fixed projection orders have computational complexity that is definitely greater than that of the proposed algorithm when the number of iterations is sufficiently large. Therefore, although the proposed algorithm increases the computational load of calculating two MSDs compared to the original algorithm, its computational complexity is still lower than that of several similar algorithms. Thus, due to the introduction of the VPO method, the proposed algorithm has significant potential for application in airborne radar signal self-interference cancellation technology due to its lower computational complexity.

Table 1 Computational complexity analysis of different algorithms

Algorithm	Multiplication	Addition
APA	$(K^2+2K)L+K^3+K$	$(K^2+2K)L+K^3+K^2-K$
APSA	$(K+2)L+1$	$(2K+1)L$
VPO-APA	$(K_n^2+2K_n+1)L+K_n^3+K_n+18$	$(K_n^2+2K_n)L+K_n^3+K_n^2-K_n+10$
EPAA	$2KL+3K$	$2KL+K$
VPO-PAPA	$(K_n^2+2K_n+4)L+K_n^3+K_n+18$	$(K_n^2+2K_n+1)L+K_n^3+K_n^2-K_n+11$
VPO-EPAA	$2K_nL+3K_n+22$	$2K_nL+K_n+4$

4 Simulation Results

In the simulation phase, the optimal values for key fixed parameters of the proposed algorithm will be determined initially. After that, the algorithm will be evaluated against several similar methods, as discussed earlier, through simulations in two scenarios: System identification and airborne radar signal self-interference cancellation. The self-interference cancellation scenario includes self-interference paths and airborne radar input signals that are affected by multipath propagation, which is a key focus in the upcoming simulations. Unless stated otherwise, the performance of the algorithm will be assessed using the normalised mean square deviation (NMSD) metric, shown as

$$\mathrm{NMSD}=10\lg\left(\frac{\|\boldsymbol{w}_0-\boldsymbol{w}(n)\|_2^2}{\|\boldsymbol{w}_0\|_2^2}\right) \tag{23}$$

A smaller difference between the system's weight vector $\boldsymbol{w}_0$ and the weight vector $\boldsymbol{w}(n)$ simulated by the algorithm results in a lower final NMSD value, indicating better algorithm performance. The algorithm's convergence speed can also be evaluated by the rate at which the NMSD decreases. Unless stated otherwise, all simulation experiments use a 30 dB Gaussian white noise input. Typically, the presented simulation curves are averaged from 200 independent experiments.

4.1 Algorithm parameter selection and theoretical verification

The simulation setup for selecting algorithm parameters is the same as that for system identification. Therefore, the configuration of the system identification environment is detailed in this section. The length of the system and filter are both set to $L=20$. The input signal in this experiment is an autoregressive (AR) signal, generated from a Gaussian white noise signal using an AR training model. The autoregressive model used in this study is defined as

$$G(z)=\frac{1+0.5z^{-1}+0.81z^{-2}}{1-0.59z^{-1}+0.4z^{-2}} \tag{24}$$

where variable z is the complex quantity that represents the signal in the frequency domain, while $G(z)$ the transfer function of the autoregressive model.

In this section, the exhaustive approach will be applied to select two crucial parameters, μ and q, for the algorithm. The parameters will be paired in

increasing order of their values. Simulation experiments will be performed for each combination, and the optimal values will be identified by comparing the steady-state errors at equivalent convergence speeds.

In the simulation experiments, the maximum projection order for the algorithm using the VPO method was set to 16, with a minimum of 1. The system elements to be identified were randomly generated within the range of −1 to 1, with a sparsity of 1/10. The remaining parameters of the proposed algorithm were configured according to Ref.[30], with a regularization parameter of $m=0.3$. The algorithm was executed for 1 500 iterations, and pulse noise with an α-stable distribution was introduced. It is crucial to note that parameters outside the experimental range may impact performance evaluation. If the step size μ is too small, it may not be possible to reach a steady state value within a given number of iterations, while if the step size is too large, the algorithm may fail to converge. A small value for parameter q reduces the algorithm's adaptability, whereas a large value may excessively amplify the effect of errors. The results for the parameter selection of the proposed algorithm are shown in Fig.1.

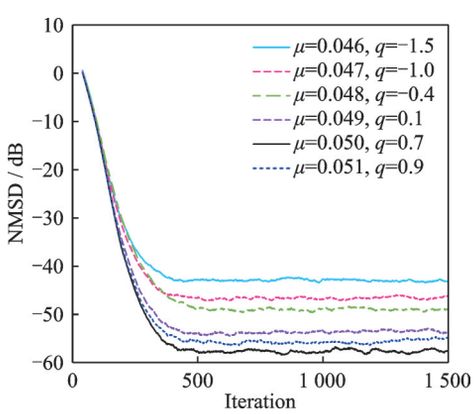

Fig.1 Performance of the algorithm proposed in this paper for different parameter combinations with a system sparsity of 1/10 (Adding impulse noise [1.9, 0, 0.003, 0])

As can be clearly seen from Fig.1, when $\mu=0.050$ and $q=0.7$, the algorithm achieves the lowest steady-state error at the same convergence rate as other parameter combinations. Therefore, these values are selected as the parameter values for subsequent experiments. Additionally, to assess the compatibility of the VPO method with the algorithm proposed in this paper, the optimal parameter values mentioned above are used as a reference to plot the variation curve of the projection order K throughout the entire simulation experiment. Since this value is an integer, the results of a single simulation experiment can more intuitively reflect its changes and stability. The simulation results of a single experiment are shown in Fig.2.

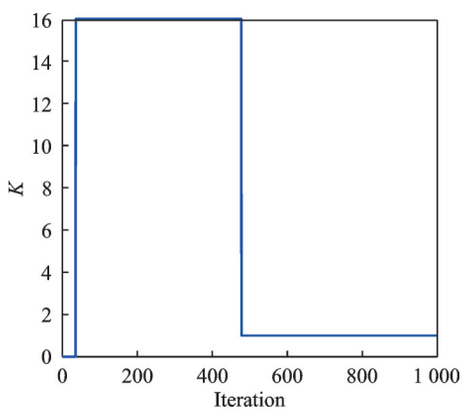

Fig.2 Simulated variation curve of the projection order K with a system sparsity of 1/10 (Adding impulse noise [1.9, 0, 0.003, 0])

As shown in Figs.1 and 2, the change curve of the K value clearly reflects the convergence of the proposed algorithm. At the beginning of the iteration, the projection order of the algorithm remains at the set maximum value of 16. As convergence occurs, the projection order of the algorithm changes from 16 to 1 and remains stable. The results of this experiment indicate that the VPO method is highly compatible with the algorithm proposed in this paper.

Additionally, to confirm the accuracy of the derivation results from the VPO method, the current NMSD value from Eq.(14) was compared with the steady-state NMSD estimate from Eq.(15) through simulation experiments. The simulation results for $K=1$ are displayed in Fig.3.

With each iteration, the two curves nearly align at the same value. Thus, the $p(n)$ value proposed in this study effectively predicts the algorithm's NMSD.

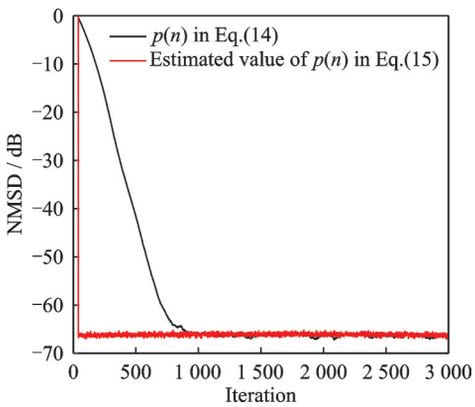

Fig.3 Comparison of the current $p(n)$ value of the algorithm with the estimated NMSD value

4.2 System identification simulation

Before performing the formal self-interference cancellation simulations, system identification tests must be conducted in different environments to ensure proper filter initialization. In this section, the algorithm presented in this paper is simulated and compared with the five algorithms discussed in the complexity analysis section. These algorithms are applicable in the same environments. To assess the algorithm's tracking performance, the simulation also includes system identification experiments in non-smooth conditions. For the system identification experiments, 1 500 iterations are carried out in smooth environments, while 9 000 iterations are executed in non-smooth environments. In non-smooth environments, the initial sparsity is 1/10, the sparsity becomes 1/2 at 3 000 iterations and the system becomes non-sparse at 6 000 iterations. For APA, the projection order is set to $K=8$ with a step size of $\mu=0.05$, and for APSA, the same values of $K=8$ and $\mu=0.05$ are applied. In VPO-APA, the step size is $\mu=0.5$, and the forgetting factor is set to $\chi=a=0.999$. The other parameters match those used in this study. In EPAA, $\mu=0.012$, the regularization parameter is $m=0.2$, and the tuning parameter is $q=0.7$. In VPO-PAPA, the forgetting factor is $\chi=a=0.999\ 9$, the tuning parameter is $\beta=-0.5$, and the other settings are consistent with the proposed algorithm. The results of the system identification experiments in both smooth and non-smooth environments are given below.

Figs.4 and 5 show the system identification in smooth and non-smooth environments with the sparsity of 1/10 and with added impulse noise [1.8, 0, 0.003, 0]. As shown in Figs.4 and 5, basic algorithms like APA and APSA perform poorly under pulse noise interference. The improved VPO-APA shows slightly lower steady-state error than EPAA but has slower convergence. Both VPO-PAPA with a proportional matrix and the proposed algorithm outperform others, as their cost function characteristics or enhanced techniques are more suitable for self-interference cancellation. The proposed algorithm, combining VPO with the Ekblom norm's robustness, demonstrates exceptional performance. In simulations of non-stationary environments, the system sparsity significantly impacts algorithm performance. VPO-PAPA with a proportional matrix and the proposed algorithm degrade as the system shifts from sparse to non-sparse, while the reference baseline is less affected. However, due to the flexibility of VPO and the Ekblom norm, the proposed algorithm maintains the lowest steady-state error and ex-

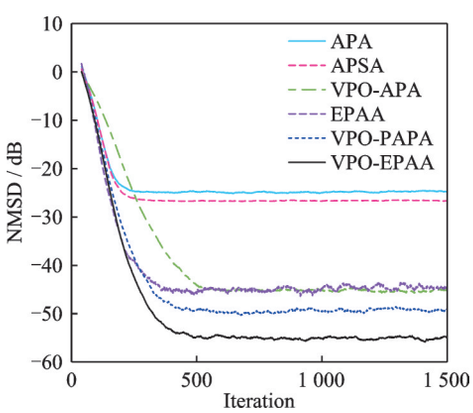

Fig.4 System identification in a smooth environment with a sparsity of 1/10 (Adding impulse noise [1.8, 0, 0.003, 0])

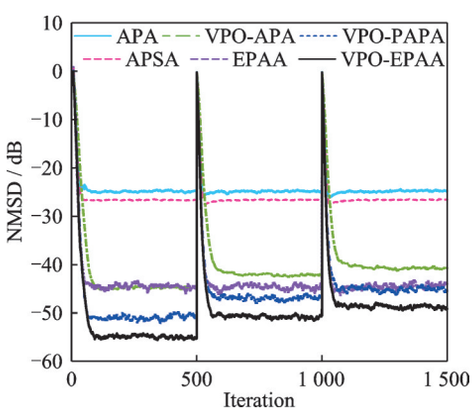

Fig.5 System identification in non-smooth environments with an initial sparsity of 1/10 (Adding impulse noise [1.8, 0, 0.003, 0])

hibits excellent tracking and fast convergence after abrupt system changes.

To evaluate algorithm robustness in challenging environments, systematic identification simulations will be conducted at varying pulse noise levels. Two sets of experiments will be performed under consistent conditions, with increasing pulse noise intensities and the results are given below.

Figs.6 and 7 show the system identification for different impulse noise intensities with the system of 1/10 and with different impulse noises. The simulation results in Figs.6 and 7 show that all algorithms are affected by increasing pulse noise intensity. EPAA outperforms VPO-APA under strong pulse noise due to the high robustness of the Ekblom norm. The proposed algorithm, combining advantages from several comparison algorithms, maintains the lowest steady-state error and shows the strongest robustness under strong pulse noise.

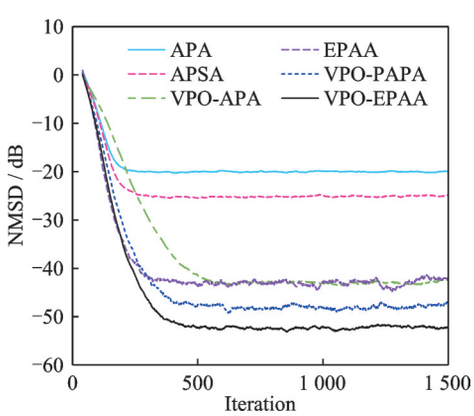

Fig.6 System identification for different impulse noise intensities with a system sparsity of 1/10(Adding impulse noise [1.6, 0, 0.003, 0])

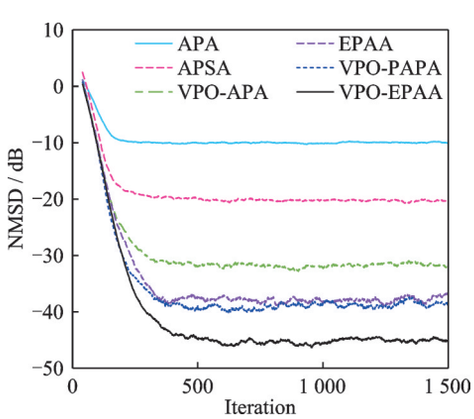

Fig.7 System identification for different impulse noise intensities with a system sparsity of 1/10(Adding impulse noise [1.2, 0, 0.003, 0])

In conclusion, the proposed algorithm demonstrates superior performance in system identification.

4.3 Self-interference cancellation simulation

In this section, the performance of the algorithm proposed in this paper will be simulated and evaluated in the context of self-interference cancellation of airborne radar signals. Fig.8 illustrates the application model for self-interference cancellation of airborne radar signals. The radar transmitter emits signals, part of which mix with external noise, creating self-interference signals re-received by a receiver on the aircraft. The path from transmission to reception is the self-interference channel. Adaptive filtering algorithms model this channel using known data, enabling accurate self-interference signal estimation and cancellation. Aircraft motion and environmental changes can cause sudden variations in the channel's impulse response.

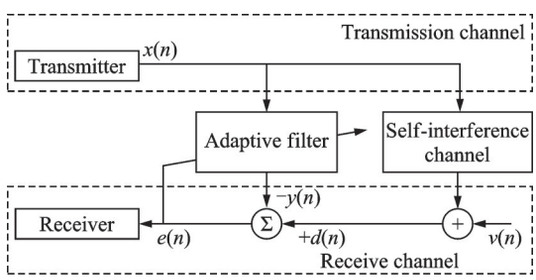

Fig.8 Self-interference cancellation scene model

The self-interference channel impulse response for simulating multipath propagation effects in airborne radar signals is shown in Fig.9.

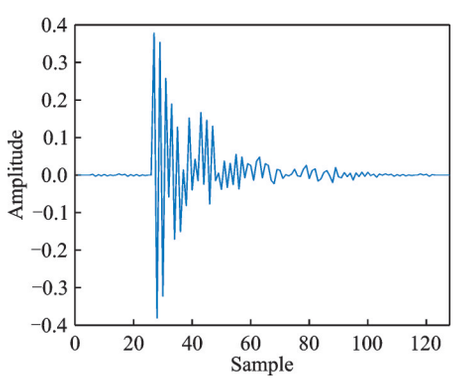

Fig.9 Impulse response of self-interference channel

The self-interference channel length is 128, with fluctuating amplitudes and multiple peaks that decrease and stabilize. This characteristic reflects the actual situation where self-interference signals are collected at different time after being reflected

through different paths. Furthermore, the parameter design of the channel to be simulated also reflects the sparsity of the operating environment of airborne radar signals. In addition, frequency-modulated continuous wave (FMCW) with a sampling frequency of 150 MHz is used as the input signal. This signal has high continuity and low transmission power, and is a commonly used type of airborne radar signal. The FMCW signal waveform used in this paper is shown in Fig.10.

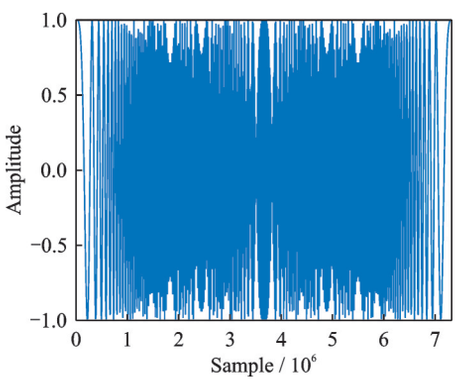

Fig.10 FMCW signal waveform

Next, simulation experiments will be conducted using several sets of noise inputs of different intensities and types in a non-stationary environment. In non-smooth environments, the system multiplies the impulse response by -1 at 1.5×10^5 iterations. The parameter settings for all algorithms are the same as those used in the system identification simulation experiments. First, self-interference cancellation experiments were conducted in both steady and non-steady environments. The simulation results are shown in Figs.11 and 12.

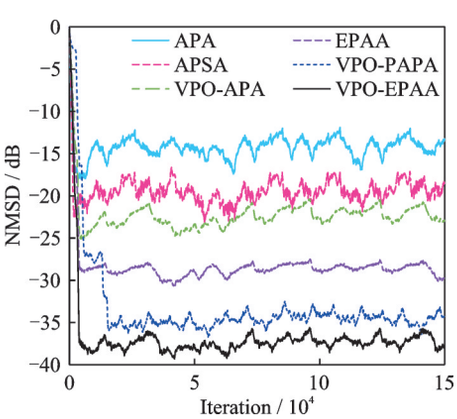

Fig.11 Self-interference cancellation simulation of six algorithms in a stationary environment(Adding impulse noise [1.4, 0, 0.003, 0])

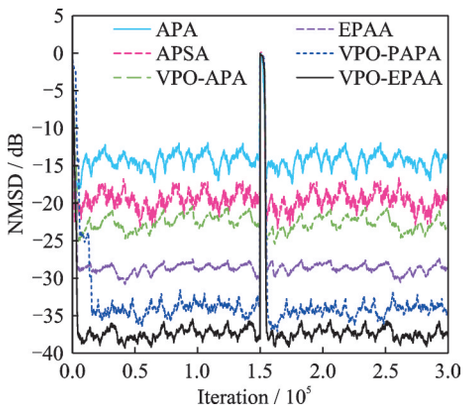

Fig.12 Self-interference cancellation simulation of six algorithms in a non-stationary environment (Adding impulse noise [1.4, 0, 0.003, 0])

As illustrated in Figs.11 and 12, due to the non-stationary characteristics of self-interference channels, all algorithms showed performance fluctuations to varying extents after convergence. The performance variations align with the outcomes of the system identification experiments. As shown in Fig.12, when the parameters of the channel to be simulated undergo sudden changes, the weight vector of the filter will be reset. Nevertheless, the new algorithm consistently achieved the lowest steady-state error, faster convergence, and higher tracking capability, highlighting its robustness in this environment.

In addition, two sets of self-interference cancellation simulation experiments with colour noise were conducted. The colour noise signal was generated from a Gaussian white noise signal with a mean of 0 and a variance of 1, and then passed through a first-order filter with a pole located at 0.9. Its waveform is shown in Fig.13.

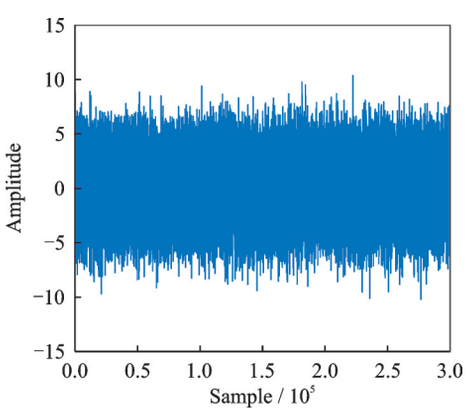

Fig.13 Colour noise signal

In the initial experiment, colour noise was applied before the abrupt change in simulated channel parameters. This noise was combined with 30 dB Gaussian white noise to create the background input noise. In these environments, the system multiplie the impulse response by -1 at 1.5×10^5 iterations. After the channel parameters changed suddenly, only Gaussian white noise remained. In the second experiment, colour noise was again used before the parameter change. After the change, pulse noise replaced the input noise. The results from both experiments are presented in Figs.14 and 15.

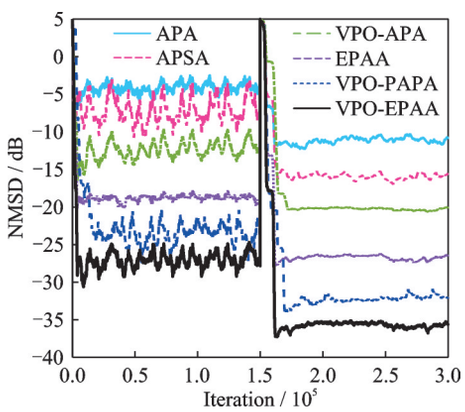

Fig.14 Self-interference cancellation simulation of six algorithms in a non-stationary environment (Gaussian white noise with a noise level of 30 dB after mutation)

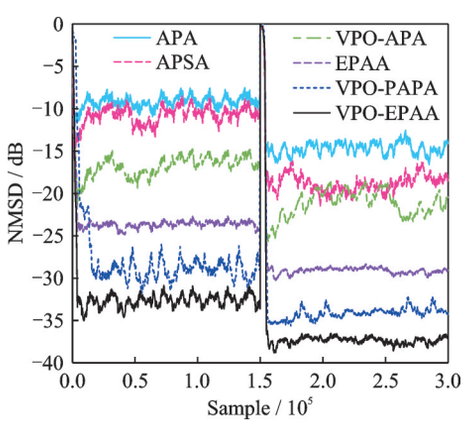

Fig.15 Self-interference cancellation simulation of six algorithms in a non-stationary environment (The noise changing to impulse noise [1.4, 0, 0.003, 0] after mutation)

The experimental results above indicate that the power spectral density characteristics of colour noise lead to a performance decline in most algorithms. Overall, the results resemble those observed under strong pulse noise conditions. All experiments highlight the robustness of the VPO method and the cost function of the proposed algorithm. In conclusion, the algorithm shows outstanding performance in complex environments with different types and levels of noise interference, suggesting its significant potential for self-interference cancellation in airborne radar applications.

5 Conclusions

This paper proposes VPO-EPAA to address the limitations of airborne radar signal self-interference elimination algorithms in terms of environmental adaptability. The algorithm incorporates a VPO mechanism utilizing the MSD method, improving the trade-off between convergence speed and steady-state error, while also reducing computational complexity. Simulation results confirm that the proposed algorithm provides the faster convergence, the lower steady-state error, and the enhanced tracking ability, along with improved robustness against both strong pulse noise and colour noise. Comparison with existing algorithms shows that the proposed algorithm outperforms several current solutions in self-interference cancellation applications in multiple areas. But simulation tests show that the performance of the algorithm deteriorates under strong interference noise conditions. Future research will focus on optimising the cost function of the algorithm to improve its robustness in the operational environment of airborne radars.

References

[1] ZHAO J, SHEN M, ZHU D, et al. Improved Doppler warping method for airborne radar with non-side-looking array[J]. Transactions of Nanjing University of Aeronautics and Astronautics, 2013, 30(2): 169-174.

[2] HU X, WANG X, QIN K, et al. Digital predistortion of nonlinear power amplifier based on improved spline adaptive filtering method[J]. IEEE Access, 2022, 10: 122870-122881.

[3] CAO R, ZHANG X. Computationally efficient MUSIC-based algorithm for joint direction of arrival (DOA) and doppler frequency estimation in monostatic MIMO radar[J]. Transactions of Nanjing University of Aeronautics and Astronautics, 2018, 35(6): 1053-

1063.

[4] FENSKE P, KOEGEL T, GHASEMI R, et al. Constellation estimation, coherent signal processing, and multiperspective imaging in an uncoupled bistatic cooperative radar network[J]. IEEE Journal of Microwaves, 2024, 4(3): 486-500.

[5] CHEN C, ZHANG Z, LIAN H. A low-complexity joint angle estimation algorithm for weather radar echo signals based on modified ESPRIT[J]. Journal of Industrial Engineering and Applied Science, 2025, 3(2): 33-43.

[6] PARK C H, CHANG J H. Shrinkage estimation-based source localization with minimum mean squared error criterion and minimum bias criterion[J]. Digital Signal Processing, 2014, 29: 100-106.

[7] WANG C, WEI Y, YUKAWA M. Dispersed-sparsity-aware LMS algorithm for scattering-sparse system identification[J]. Signal Processing, 2024, 225: 109616.

[8] BERSHAD N J, BERMUDEZ J C M. Modified LMS and NLMS algorithms with non-negative weights[J]. Signal Processing, 2024, 223: 109567.

[9] ZHOU X, LI G, WANG Z, et al. Robust hybrid affine projection filtering algorithm under α-stable environment[J]. Signal Processing, 2023, 208: 108981.

[10] PATEL V, BHATTACHARJEE S S, JENSEN J R, et al. Nonlinear acoustic echo cancellation using low-complexity low-rank recursive least-squares algorithms[J]. Signal Processing, 2024, 225: 109623.

[11] ZENG X, LV R, LI S. The maximum a posteriori estimation model for signal recovery with mixed Gaussian and impulse noise[J]. Applied Mathematics Letters, 2024, 147: 108859.

[12] HOU X, ZHAO H, LONG X, et al. Computationally efficient robust adaptive filtering algorithm based on improved minimum error entropy criterion with fiducial points[J]. ISA transactions, 2024, 149: 314-324.

[13] HOU Y, LI G, ZHANG H, et al. Affine projection algorithms based on sigmoid cost function[J]. Signal Processing, 2024, 219: 109397.

[14] LIU C, ZHANG Z, TANG X. Sign normalised spline adaptive filtering algorithms against impulsive noise[J]. Signal Processing, 2018, 148: 234-240.

[15] KIM S H, JEONG J J, CHOI J H, et al. Variable step-size affine projection sign algorithm using selective input vectors[J]. Signal Processing, 2015, 115: 151-156.

[16] FOURNIER D, OLDENBURG D W. Inversion using spatially variable mixed l_p norms[J]. Geophysical Journal International, 2019, 218(1): 268-282.

[17] HUANG X, LI Y, HAN X, et al. Ekblom promoting adaptive algorithm for system identification[J]. Signal Processing, 2023, 203: 108797.

[18] KOLODZIEJ K E, PERRY B T, HERD J S. In-band full-duplex technology: Techniques and systems survey[J]. IEEE Transactions on Microwave Theory and Techniques, 2019, 67(7): 3025-3041.

[19] ERDEM M, OZKAN H, GURBUZ O. A new online nonlinear self-interference cancellation method with random fourier features[J]. IEEE Wireless Communications Letters, 2022, 11(7): 1379-1383.

[20] YU Y, ZHAO H, CHEN B. Steady-state mean-square-deviation analysis of the sign subband adaptive filter algorithm[J]. Signal Processing, 2016, 120: 36-42.

[21] LI K, YU Y, HE H, et al. Novel normalized subband adaptive filtering algorithms with weights-dependent variable step-size[J]. Digital Signal Processing, 2025, 158: 104945.

[22] VOGT H, ENZNER G, SEZGIN A. State-space adaptive nonlinear self-interference cancellation for full-duplex communication[J]. IEEE Transactions on Signal Processing, 2019, 67(11): 2810-2825.

[23] ZHANG J, HE F, LI W, et al. Self-interference cancellation: A comprehensive review from circuits and fields perspectives[J]. Electronics, 2022, 11(2): 172.

[24] LIU C, JIANG M. Robust adaptive filter with lncosh cost[J]. Signal Processing, 2020, 168: 107348.

[25] ZHOU Y, ZHAO H, ZHU Y. Robust generalized hyperbolic secant algorithm for nonlinear active noise control[J]. Applied Acoustics, 2023, 209: 109422.

[26] BAHRAINI T, SADIGH A N. Proposing a robust RLS based subband adaptive filtering for audio noise cancellation[J]. Applied Acoustics, 2024, 216: 109755.

[27] SHANG N, XIN K, YU C J, et al. Design of direct wave cancellation system for high-frequency CW radar[J]. Journal of Engineering-Joe, 2019, 2019(20): 6660-6663.

[28] LI H, GAO Y, GUO X, et al. Variable-step-size generalized maximum correntropy affine projection algorithm with sparse regularization term[J]. Electronics, 2025, 14(2): 291.

[29] WANG X, OU S, GAO Y. Convex regularized recursive minimum error entropy algorithm[J]. Electronics, 2024, 13(5): 992.

[30] LUO L, YU Y, YANG T, et al. Affine projection algorithms with novel schemes of variable projection order[J]. Circuits, Systems, and Signal Processing, 2024, 43(12): 8074-8090.

Acknowledgement This work was supported by the Shandong Provincial Natural Science Foundation (No. ZR2022MF314).

Authors

The first author Mr. **LI Haorui** obtained a Bachelor of Engineering degree from Shandong Jianzhu University in 2023. Since 2023, he has been studying at School of Physics and Electronic Information at Yantai University. His research field is intelligent information systems.

The corresponding author Prof. **OU Shifeng** obtained his B.S. degree in electronic information engineering from School of Communication Engineering at Jilin University in 2002 and his Ph.D. degree in communication and information systems from the same institution in 2008. Since 2008, he has been employed at School of Physics and Electronic Information at Yantai University, where he currently holds the position of Professor. His research focuses primarily on intelligent speech signal processing and blind signal processing.

Author contributions Mr. **LI Haorui** designed the research plan, constructed the model, performed data analysis, interpreted the research results, and wrote the paper. Prof. **GAO Ying** provided data on the radar signal self-interference cancellation model. Mr. **GUO Xinyu** provided analysis of the simulation experiment data. Prof. **OU Shifeng** participated in the discussion and background section of the research, as well as the revision of the initial draft of the paper. All authors commented on the manuscript draft and approved the submission.

Competing interests The authors declare no competing interests.

(Production Editor: SUN Jing)

可变投影阶数的自适应滤波算法在机载雷达中的自干扰对消应用

李浩瑞[1], 高 颖[1], 郭鑫宇[2], 欧世峰[1]

(1.烟台大学物理与电子信息学院,烟台 264005,中国;
2.吉林大学仪器科学与电气工程学院地球信息探测仪器教育部重点实验室,长春 130000,中国)

摘要: 具有固定投影阶数的自适应滤波算法无法根据机载雷达外部环境的变化调整其性能。为克服这一局限性,本文提出了一种可变投影阶数的Ekblom范数促进自适应算法(Variable projection order Ekblom norm-promoted adaptive algorithm, VPO-EPAA)。该方法首先分析原EPAA的均方偏差(Mean squared deviation, MSD),并推导出其MSD的计算公式。通过比较EPAA在两种不同投影阶数下的MSD,选择使MSD最小的投影阶数作为当前迭代的算法参数。此外,本文也对新算法的计算复杂度进行了理论分析。系统辨识与自干扰对消实验的仿真结果表明,本文所提算法在机载雷达信号自干扰对消方面表现优异,即使在不同强度和类型的噪声干扰下也能发挥较高性能。

关键词: 自适应滤波算法;机载雷达;可变投影阶数;均方偏差;自干扰对消